



ELSEVIER

Nuclear Instruments and Methods in Physics Research B 174 (2001) 433–438

NIM B
Beam Interactions
with Materials & Atoms

www.elsevier.nl/locate/nimb

Algorithm for statistical noise reduction in three-dimensional ion implant simulations

J.M. Hernández-Mangas^{*}, J. Arias, M. Jaraiz, L. Bailón, J. Barbolla

Dept. Electricidad y Electrónica, Universidad de Valladolid, 47011 Valladolid, Spain

Received 25 July 2000; received in revised form 10 October 2000

Abstract

As integrated circuit devices scale into the deep sub-micron regime, ion implantation will continue to be the primary means of introducing dopant atoms into silicon. Different types of impurity profiles such as ultra-shallow profiles and retrograde profiles are necessary for deep submicron devices in order to realize the desired device performance. A new algorithm to reduce the statistical noise in three-dimensional ion implant simulations both in the lateral and shallow/deep regions of the profile is presented. The computational effort in BCA Monte Carlo ion implant simulation is also reduced. © 2001 Elsevier Science B.V. All rights reserved.

PACS: 82.20.Wt; 61.72.Tt; 34.10.+x

Keywords: Ion implantation; Computer simulation; Rare event

1. Introduction

As semiconductor devices decrease in size, previously negligible two-dimensional effects have become much more important, greatly increasing the need for understanding two-dimensional dopant distributions. The ability to accurately predict the lateral doping profiles as well as the depth profiles in a computationally efficient manner is important for optimum design and fabrication of

advanced devices and circuits. Also the dopant profiles implanted with high energies in order to get retrograde wells are important. The retrograde doping profiles serve the needs of channel engineering in deep submicron MOS devices for punch-through suppression and threshold voltage control. Therefore, a correct description of the shallow side of the impurity profiles is needed. The International Technology Roadmap for Semiconductors [1] calls for a self-consistent hierarchy of tools that allows for a trade-off between speed and accuracy.

In order to obtain good simulation results under channeling conditions [6–8], the inelastic energy loss must be divided into two components: a *local* and a *non-local* contribution. It is found

^{*} Corresponding author. Tel.: +34-983-423000 ext. 25506; fax: +34-983-423675.

E-mail address: jesman@ele.uva.es (J.M. Hernández-Mangas).

necessary [2] to include energy loss due to inelastic collisions (*local*), and energy loss due to electronic stopping (*non-local*) as two distinct mechanisms. It is not possible to assume that one, or other, of these processes is dominant and *fit* it to model all energy loss for varying energies and directions.

The *non-local* inelastic stopping accounts for the energy loss of the ion as it travels along the interstitial volume of the target. It is due to the interaction between the nucleus of the projectile and the target's electrons. This electronic stopping is given by the modified Brandt–Kitagawa [3] theory with only one adjustable parameter r_s^0 [4,5] and is calculated as

$$S_e = \int [Z_1^*(v, r_s^0)]^2 S_p(v, r_s) dx, \quad (1)$$

where Z_1^* represents the effective charge of the ion and depends on r_s^0 , that is related with the effective electron density of the target and depends on the ion–target combination [4]; v is the ion velocity; $r_s = (3/(4\pi\rho))^{1/3}$ the one-electron radius (ρ is the local electron density) and S_p the electronic stopping power for a proton [9] that depends on the local electron density accounting for the crystalline structure of the target. A numerical-efficient approximation to the Echenique theory [9] is used. A three-dimensional electron charge distribution for the silicon, that includes the covalent tetrahedral bonds, is calculated by the ab initio pseudo-potential total energy method in the local density approximation [10] and gives an accurate description of channeling effects [6].

The *local* inelastic stopping is related with the close collisions and takes into account the electron–electron interaction between ion and target. It is described by the modified Firsov theory [11,12] as proposed by Cai et al. [4]:

$$F_{ij} = \frac{2^{1/3}\hbar}{2\pi a_B} (\hat{v}_j - \hat{v}_i) \times \left[Z_1^2 I \left(\frac{Z_1^{1/3} \alpha R}{a} \right) + Z_2^2 I \left(\frac{Z_2^{1/3} (1 - \alpha) R}{a} \right) \right], \quad (2)$$

where

$$I(X) = \int_X^\infty \frac{\chi^2(x)}{x} dx, \quad (3)$$

$$\alpha = \left[1 + \left(\frac{Z_2}{Z_1} \right)^{1/6} \right]^{-1}$$

and $\chi(x)$ is the universal screening function [13], Z is atomic number ($Z_1 > Z_2$), R is atomic separation, $a = (9\pi^2/128)^{1/3} a_B$ and a_B the Bohr radius.

In order to reduce the calculation time and to improve the accuracy of the simulated profiles a three-dimensional rare event algorithm is implemented. The number of cascades simulated to get a good statistic profile depends on the desired number of orders of magnitude of accuracy. If we want to calculate a statistically significant concentration at all depths or zones of the profile we will have to run many ions that are stopped near the peak for every ion that stops in the tail or in any low concentration zone, and most of the computer effort will not improve the accuracy of the profile being generated.

2. Algorithm description

There have been several attempts in the past to improve the efficiency of the ion implant simulators. Yang et al. [14] proposed a rare event approach but it needs several separated simulations and does not have a defined mechanism to choose neither how many simulations nor the depths to split the projectiles. Beardmore et al. [2] proposed a rare event algorithm that solves the problems encountered in Yang's approach, but it only improves the statistical noise in the deep region of the profile. Bohmayr et al. [15] developed a different trajectory split method based in checking the local dopant concentration at certain points. It uses a complex three-dimensional octree. The virtual trajectories are not splitted recursively and consequently the maximum performance of the algorithm is not achieved. Schmidt et al. [16,17] implemented for two-dimensional profiles a splitting algorithm that only improves the depth resolution. It is very memory consuming storing the positions of neighboring target atoms and the

particle trajectory density at each triangular cell. Also the computation time is still considerable.

A method to overcome these limitations is proposed. All of these algorithms implement an atom splitting scheme so that at certain depths the ion is split into two virtual ions with a statistical weight of half the unsplit ion. The virtual ions generated have the same position and velocity as the parent ion. Their final trajectories are, however, different due to the thermal vibration effects.

In order to reduce the statistical noise of the simulated profiles, we need, first at all, to identify the rare events. In the ion implant simulation there are two cases of particular interest:

1. *Channeled ions.* This case occurs when the ion travels through a crystal channel. It loses its energy mainly by inelastic interaction without having hard nuclear (elastic) collisions. We can identify these ions by monitoring their depth from the surface. If we want to improve also the statistics of the laterally channeled ions, we will monitor the total distance traveled by the ion.
2. *Projectiles in the shallow region of the impurity profile.* These ions have probably lost most of their energy in a few hard nuclear collisions at the beginning of their flight. They have relatively low energy and are near the surface. This case is only important when we simulate high energy implants.

2.1. Statistical noise reduction in the deep/lateral zones

An accurate description without statistical noise in the lateral regions of the two-dimensional profiles is now becoming necessary. We define, in general, a border d_i as either a depth reached by the ion or as the total distance traveled by the ion. We can choose the behaviour of our algorithm in order to improve only the deep zone or – in a general way – the lateral and deep zones. When the ion reaches the border with the next index, it is splitted into two virtual ions with half statistical weight. In Fig. 1, we can see an example of how a real ion is splitted several times into several virtual ions when it reaches certain borders. We show also the statistical weight associated with each virtual ion.

The borders cited above are calculated by solving the following equation:

$$\int_0^{d_i} C(x) dx = (1 - (1/2)^i) \int_0^\infty C(x) dx, \quad (4)$$

where $C(x)$ is the dopant histogram profile at a certain depth (or total distance traveled) x .

With this scheme we can recalculate the splitting borders dynamically in order to improve the statistics in specific regions. We do not need to know a priori the borders. First, N_0 real ions are simulated without the rare event algorithm, in order to obtain some statistics to estimate the

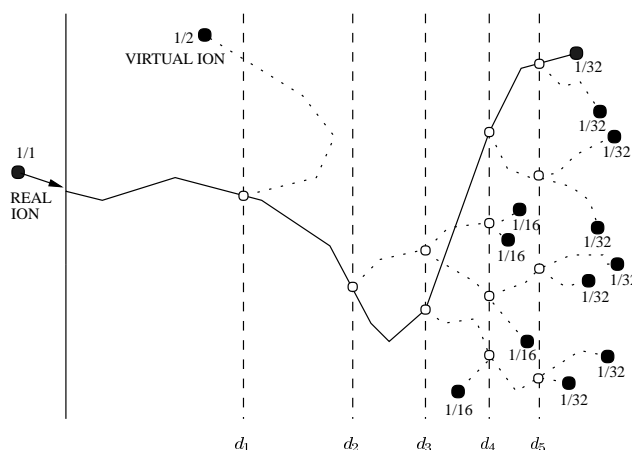


Fig. 1. Rare event algorithm with lateral or depth enhancement scheme.

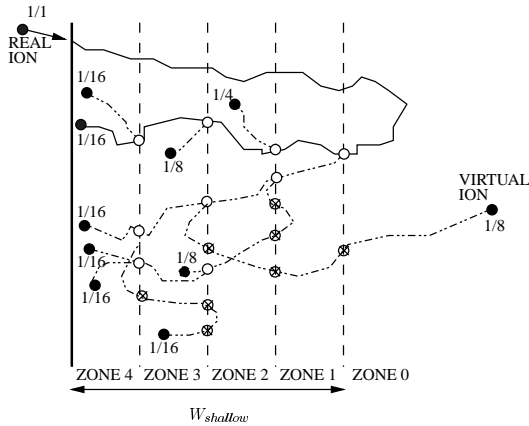


Fig. 2. Rare event algorithm with shallow region enhancement scheme.

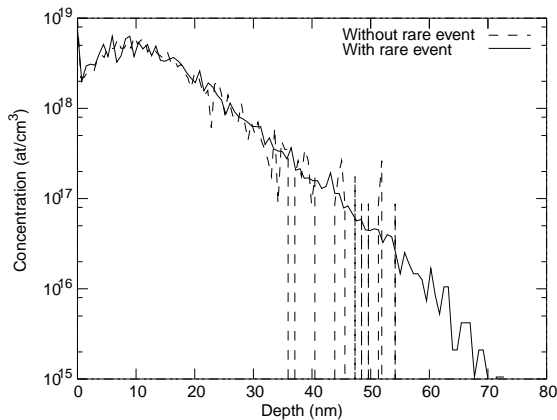


Fig. 3. Implantation of B (tilt = 7°, rotation = 30°) → Si {100}, 2 keV simulated with $N_{\text{ion}} = 2000$ real ion with and without the trajectory-length selection scheme.

borders d_i . Then, the algorithm is activated and every N_{interval} real ions the borders are recalculated. This value must be large enough (i.e. $N_{\text{interval}} = 100$) not to increase the computation time. When we have reached the desired statistical accuracy in the rare event region the algorithm is automatically deactivated.

2.2. Statistical noise reduction in the shallow region of the profiles

When we simulate medium and high energy implants there is some statistical noise in the shallow region of the profiles due to the (few) ions who have lost their energy at the beginning of their travel. We can select these cases to apply a specific rare event algorithm. There are two conditions:

1. *An energy condition:* the energy decreases below a user defined threshold energy, $E \leq E_{\text{th}}$, that is generally a percentage of the initial energy. Ions that verify this condition are likely to stop nearby.

2. *A positional condition:* We consider the shallow region (Fig. 2) defined by

$$W_{\text{shallow}} = p_d(D_{\text{max}} - D_{\text{min}}), \quad (5)$$

where D_{max} is the maximum depth reached by an implanted ion, D_{min} is the positive minimum depth of the current profile and p_d is the percentage of the whole profile that the user considers to be the shallow region. We divide W_{shallow} into N equal zones. Initially the projectile is considered to have index 0 ($n_{\text{index}} = 0$, with unity statistical weight). When the first condition ($E \leq E_{\text{th}}$) is met we com-

Table 1

Simulation of B (7°,30°) → Si {100}, 2 keV. CPU time comparison using the different algorithms and with different numbers of real ions. Run on a 400 MHz Alpha 21164 CPU

	Time (s)	Real ions	Virtual ions	Extra decades of accuracy	Time factor
No algorithm (Fig. 3, dashed line and Fig. 4(a))	323	2000	–	–	1.0
No algorithm	3169	20000	–	1	9.8
Depth (one-dimensional) enhanced algorithm only (Fig. 3, solid line and Fig. 4(b))	619	2000	6325	2	1.9
Lateral (three-dimensional) enhanced algorithm only (Fig. 4(c))	1178	2000	12450	2	3.6

pare the current depth of the projectile, $D_{\text{projectile}}$, with the border that defines the next index as shown in the equation below:

$$D_{\text{projectile}} < D_{\text{min}} + W_{\text{shallow}} \left(1 - \frac{n_{\text{index}}}{N} \right). \quad (6)$$

If these two conditions are met we split the current ion into two virtual half-weighted ions and we increment n_{index} . And the same procedure is applied to both virtual ions again. Finally, the algorithm is deactivated when the statistical accuracy required is reached.

Fig. 2 illustrates an example of how the ions are splitted within this scheme when they have an energy below the selected threshold energy.

3. Results

In order to show the performance of the algorithms we present several simulations. Fig. 3 shows the results obtained with and without the trajectory-length selection scheme for a simulation of 2 keV B (tilt = 7°, rotation = 30°) → Si{1 0 0} with 2000 real ions. The two extra orders of accuracy obtained have only required to multiply by 3.6 the calculation time (see Table 1) whereas the time required to resolve just one extra order of magnitude in the profile without using the algorithm is ten times longer.

Fig. 4(a) shows the two-dimensional profile simulated without using the rare event algorithm, Fig. 4(b) uses Beardmore’s [2] depth selection scheme and Fig. 4(c) was calculated using the new trajectory-length selection scheme. We can see the reduction of statistical noise in the lateral regions

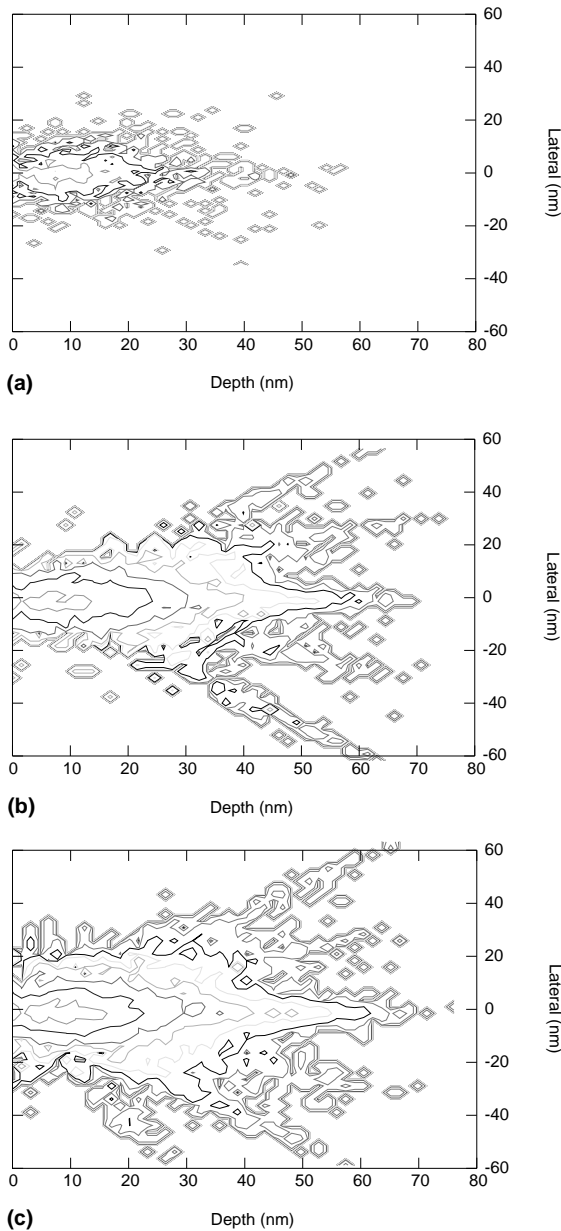


Fig. 4. Two-dimensional profile for an implantation of B (7°,30°) → Si {1 0 0}, 2 keV ($N_{\text{ion}} = 2000$ real ion): (a) without using the algorithm, (b) using the depth selection rare event algorithm, (c) using the trajectory-length selection rare event algorithm.

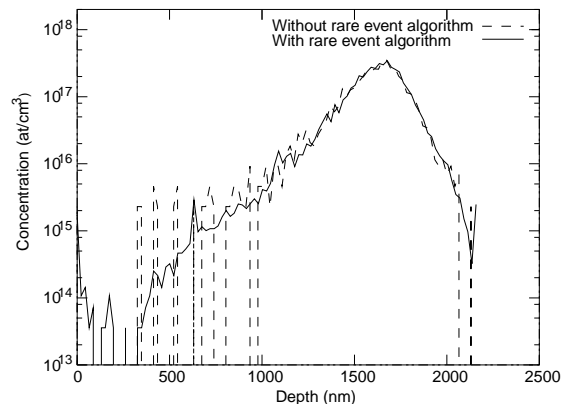


Fig. 5. Profile comparison for an implantation of B (7°,30°) → Si {1 0 0}, 1 MeV.

Table 2

Simulation of $B(7^\circ, 30^\circ) \rightarrow Si\{100\}$, 1 MeV. CPU time comparison with or without using the complete rare event enhanced algorithm. Run on an eight 400 MHz Alpha 21164 CPU cluster with the parallel version of the simulator

	Time (s)	Real ions	Virtual ions	Extra decades of accuracy	Time factor
No algorithm (Fig. 5, dashed line)	4828	2000	–	–	1.0
No algorithm	36929	20000	–	1	7.6
With shallow algorithm (Fig. 5, solid line)	7322	2000	6287	2	1.5

when we use the trajectory-length selection scheme. The calculation time increases a factor of four, as shown in Table 1, when we use our new scheme, resulting in an increase of accuracy by two orders of magnitude.

The result using the second rare event algorithm to improve the statistics in the shallow region is shown in Fig. 5. We have simulated a typical high energy implant to make retrograde p-wells with 1 MeV boron ($7^\circ, 30^\circ) \rightarrow Si\{100\}$ for 2000 real ions ($E_{th} = 0.1E_{initial}$ and $p_d = 0.4$). The increase in time, as shown in Table 2, is less than a factor of two and yet the reduction of statistical noise is by more than two orders of magnitude. Without using the rare event algorithm the calculation time would have to be increased by a factor of eight in order to improve the accuracy by only one order of magnitude.

4. Conclusions

A three-dimensional rare event algorithm that incorporates two new improvements is developed. First, we improve the statistics in the shallow side of one-dimensional profiles. Applications for shallow and retrograde-well profiles are shown. Also in two- and three-dimensional profiles we improve the statistics in the lateral regions. The CPU time necessary to obtain a certain accuracy is thus greatly reduced.

Acknowledgements

This work was performed under the auspices of the Junta de Castilla y León (VA 14/00B) and the DGICYT project No. PB 98-0398.

References

- [1] International Technology Roadmap for Semiconductors. Semiconductor Industry Association, 1997.
- [2] K.M. Beardmore, N. Gronbech-Jensen, Phys. Rev. E 57 (6) (1998) 7278.
- [3] W. Brandt, M. Kitagawa, Phys. Rev. B 25 (9) (1982) 5631.
- [4] David Cai, N. Gronbech-Jensen, C.M. Snell, K.M. Beardmore, Phys. Rev. B 54 (23) (1996) 17147.
- [5] D. Cai, C.M. Snell, K.M. Beardmore, N. Gronbech-Jensen, Int. J. Mod. Phys. C 9 (3) (1998) 459.
- [6] J.M. Hernández-Mangas, M. Jaraiz, J. Arias, L. Bailón, J. Barbolla, A. Rubio, 2000, unpublished.
- [7] J. Hernández, M. Jaraiz, J. Arias, L. Bailón, J. Barbolla, A. Rubio, J.L. Orantes, Conferencia de Dispositivos Electrónicos, Madrid, 1999.
- [8] J. Hernández, M. Jaraiz, J. Arias, J. Barbolla, L. Bailón, A. Rubio, Mat. Res. Soc. Symp., San Francisco, 1998.
- [9] P.M. Echenique, R.M. Nieminen, R.H. Ritchie, Solid State Commun. 37 (1981) 779.
- [10] Angel Rubio, Private communication.
- [11] L.M. Kishinevskii, Bull. Acad. Sci. USSR, Phys. Ser. 26 (1962) 11433.
- [12] O.B. Firsov, Sov. Phys. JETP 36 (1959) 1076.
- [13] J.F. Ziegler, J.P. Biersack, U. Littmark, Pergamon, New York, 1985.
- [14] S.H. Yang, S. Morris, S. Tian, K. Karab, A.F. Tasch, P.M. Echenique, R. Capaz, J. Joannopoulos, Mat. Res. Soc. Symp., 1995.
- [15] W. Bohmayr, A. Burenkov, J. Lorenz, H. Ryssel, S. Selberherr, IEEE Trans. Semic. Manuf. 8 (4) (1995) 402.
- [16] B. Schmidt, M. Posselt, N. Strecker, T. Feudel, Comput. Mater. Sci. 11 (2) (1998) 87.
- [17] B. Schmidt, M. Posselt, N. Strecker, T. Feudel, Mat. Res. Soc. Symp. 490 (1998) 21.